PROCEEDINGS OF SCIENCE

NLO QCD corrections to $pp \to e^+\nu_e\mu^+\nu_\mu jj$ in vector-boson fusion at the LHC

Lucia HOŠEKOVÁ*
Instituto de Física Corpuscular, Universitat de València - Consejo Superior de Investigaciones Científicas,
Parc Científic, 46980 Paterna (Valencia), Spain
E-mail: lucia.hosekova@ific.uv.es

We report on studies of next-to-leading order (NLO) QCD corrections to the process $pp \to e^+\nu_e\mu^+\nu_\mu jj$ which is associated with vector-boson fusion (VBF) production of an intermediate W^+W^+ pair. The impact of *s*-channel diagrams and interference contributions in VBF kinematics is analyzed at leading order (LO) and found to be entirely negligible. The NLO corrections are around 5% of the LO cross section, and the scale dependence is reduced to about 1%. We introduce a dynamic scale which improves the *K* factor in the high-energy tails of the distributions.

The European Physical Society Conference on High Energy Physics
18-24 July, 2013
Stockholm, Sweden

*Speaker.

PoS(EPS-HEP 2013)429

1. Introduction

VBF processes at the Large Hadron Collider (LHC), due to their unique signature formed by two tagging jets in the forward and backward region of the detector, offer interesting possibilities for discovery and exploring properties of the Higgs boson, testing electroweak symmetry breaking and for various searches for new physics.

We focus on the process involving the scattering of two positively charged W bosons via VBF with subsequent leptonic decay, leading to a final state with two jets, two positively charged leptons and two neutrinos at LO, i.e. $pp \to W^+W^+jj + X \to e^+\nu_e\mu^+\nu_\mu jj + X$ with a distinct signature of same-sign high-p_T leptons, missing energy and extra jets. We are specifically interested in the electroweak (EW) production mode of the order α_{EW}^6 which includes genuine VBF diagrams where the scattering weak gauge bosons are emitted from the incoming (anti-)quarks. We include both resonant contributions where the final-state leptons are produced via vector-boson decay as well as non-resonant ones.

The work presented in this report represents an independent calculation and verification of Ref. [1], and includes an assessment of the *s*-channel and interference contributions at LO. More details on the computational aspects of the calculation, and a comprehensive discussion of the numerical results and differential distributions of kinematical observables, can be found in Ref. [2].

2. Technical aspects

From computational standpoint, the reactions of type $pp \to 4ljj + X$ pose a challenging problem due to large number of contributing diagrams. Our strategy for dealing with the increased complexity lies in creating a database of building blocks and taking advantage of the fact that the EW and QCD parts of the diagrams are largely independent of one another.

Due to the fact that LHC experiments are conducted at TeV energies, fermion mass effects are strongly suppressed and have been neglected in this calculation. Furthermore, the contributions from the third-generation quarks and leptons is expected to be small [2] and have also been neglected, which allows us to approximate the CKM matrix by a unit matrix provided the interferences between kinematic channels as well as the *s*-channel contributions are negligible [3].

In order to create the building block database, all contributing diagrams are factorized by inserting the polarization sums for off-shell massive gauge bosons

$$g^{\mu\nu} = -\sum_{i=\{+,-,0\}} \varepsilon_i^{\mu}(k)\varepsilon_i^{*\nu}(k) + \frac{k^\mu k^\nu}{k^2} \tag{2.1}$$

in place of internal vector bosons connecting the EW and QCD sections of the diagrams (gauge-boson mass in the definition of longitudinal polarization vectors is replaced by $\sqrt{k^2}$). This method allows us to reuse the building blocks in multiple instances, in particular the EW blocks which are not effected by QCD corrections and can be quite complicated by themselves.

Figure 1 shows an example of a contributing diagram at LO split into four building blocks by

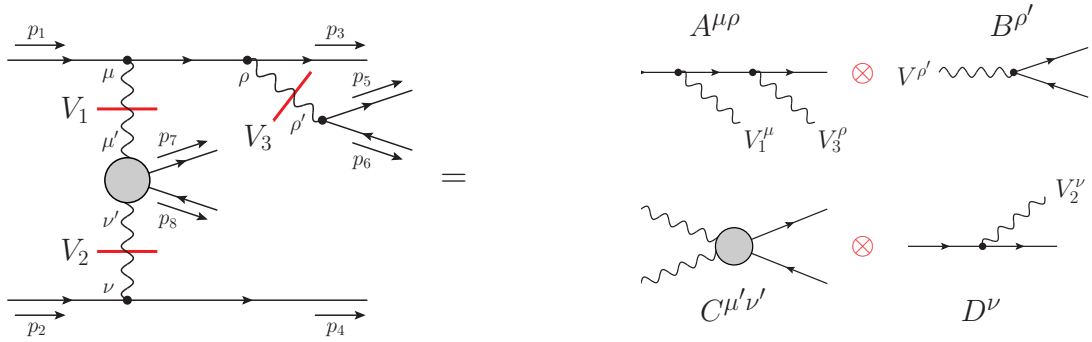

Figure 1: Example of a LO diagram split into four building blocks by applying the polarization sums (2.1) to cut three intermediate vector bosons.

inserting three polarization sums. The resulting amplitude can be written as

$$-\sum_{i,j,k=\pm,0,m} [A^{\mu\rho}\varepsilon^*_{i,\mu}(k_1)\varepsilon^*_{k,\rho}(k_3)]\,[B^{\rho'}\varepsilon_{k,\rho'}(k_3)]\,[C^{\mu'\nu'}\varepsilon_{i,\mu'}(k_1)\varepsilon_{j,\nu'}(k_2)]\,[D^{\nu}\varepsilon^*_{j,\nu}(k_2)] \times \frac{1}{k_1^2-M_{V_1}^2}\,\frac{1}{k_2^2-M_{V_2}^2}\,\frac{1}{k_3^2-M_{V_3}^2}, \tag{2.2}$$

where we have denoted $\varepsilon^\mu_m(k) = \frac{k^\mu}{\sqrt{k^2}}$ and $\varepsilon^{*\mu}_m(k) = -\frac{k^\mu}{\sqrt{k^2}}$ in order to compactify the expression. $1/(k_i^2 - M_{V_i}^2)$ are denominator parts of the split gauge boson propagators.

The expressions for individual building blocks are obtained using the FORMCALC 6 package [4], modified to accommodate the form (2.2) and exported into FORTRAN modules, while the formulas for combining the blocks are implemented as FORTRAN subroutines. At NLO, the virtual corrections lead to tensor integrals given by two- to five-point functions. Tensor reduction is performed numerically in FORTRAN by the means of the COLLIER library [5, 6, 7, 8, 9, 10]. Infrared divergencies are controlled using the Catani–Seymour dipole-subtraction technique for massless particles [11], while the ultraviolet divergencies are renormalized by adding corresponding counterterms. The FORTRAN code for each process is contained in a single function which is called from within a Monte Carlo program originally developed for the calculation published in Ref. [12]. For practical reasons, we used the tree-level amplitudes generated with OPENLOOPS [13] after cross-checking them against the ones obtained in the approach described above. The virtual amplitudes, on the other hand, are constructed using the building-block method.

Correctness of the calculation has been verified by comparing with available results and tools at both LO and NLO. Matrix elements have been compared with MADGRAPH 4 [14], OPENLOOPS [13] and stand-alone FORMCALC 6 [4] combined with LOOPTOOLS for a set of phase-space points.

We have reproduced the calculation of the full integrated cross section for the NLO QCD corrections to $pp \to e^+\nu_e\mu^+\nu_\mu jj + X$ published in Ref. [1] with the same setup and input parameters. Assuming a statistical error of the results of Ref. [1] of per-mille (it is stated to be at the sub-per-mille level), the difference amounts to only 2σ and is thus acceptable. More detailed discussion of this comparison can be found in Ref. [2].

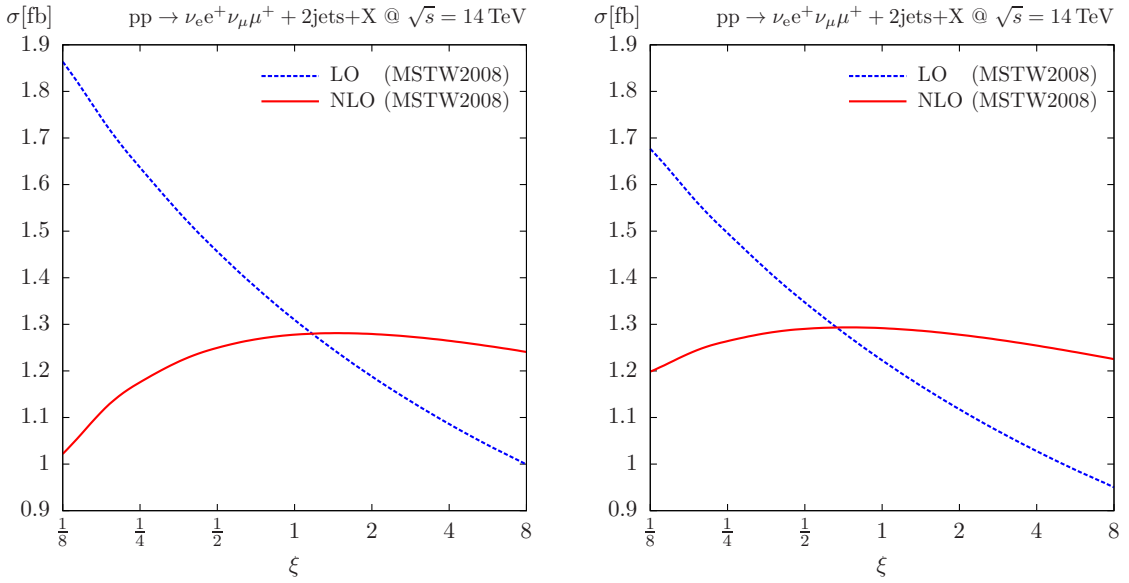

(a) $\mu_F = \mu_R = \xi M_W$ (b) $\mu_F = \mu_R = \xi \sqrt{p_{T,jet_1} \cdot p_{T,jet_2}}$

Figure 2: Scale dependence of the LO (dotted blue line) and NLO (solid red line) cross section for the fixed (a) and dynamic scale (b) as a function of the scale parameter ξ.

3. Numerical results

In order to enhance regions of the phase-space where VBF-type processes can be observed experimentally, we impose a number of kinematic cuts at the Monte Carlo level. Following the proposal in Ref. [1], these include two hard jets with large rapidity separation and charged final-state leptons located in the central detector region and separated from the jet activity. The complete set of cuts is listed in Ref. [2].

We have chosen two types of scales to demonstrate their effects on the behaviour of the NLO distributions for selected observables. In the fixed-scale (FS) choice, both factorization and renormalization scales have been set to the mass of the W boson and varied by a factor ξ around this central value,

$$\mu_F = \mu_R = \xi M_W. \tag{3.1}$$

Since this FS choice turns out to result in strongly phase-space dependent K factors—in particular in the high-energy tails of distributions—a dynamical scale (DS),

$$\mu_F = \mu_R = \xi \sqrt{p_{T,j_1} \cdot p_{T,j_2}}. \tag{3.2}$$

has been considered as well. The dependence of the total cross section on the parameter ξ for both scale choices is depicted in Figure 2. The scale variation of the LO cross section which only depends on ξ via μ_F is about $\pm 10\%$, while at NLO it is reduced to about $\pm 2\%$ of the total cross section for the FS choice and $\pm 1\%$ for the DS choice.

Dedicated VBF cuts prefer t- and u-channel kinematics, while the s-channel configurations as well as interferences between t and u channels are strongly suppressed. It can be argued [1] that these contributions can be safely neglected. In order to demonstrate this claim, the LO cross section

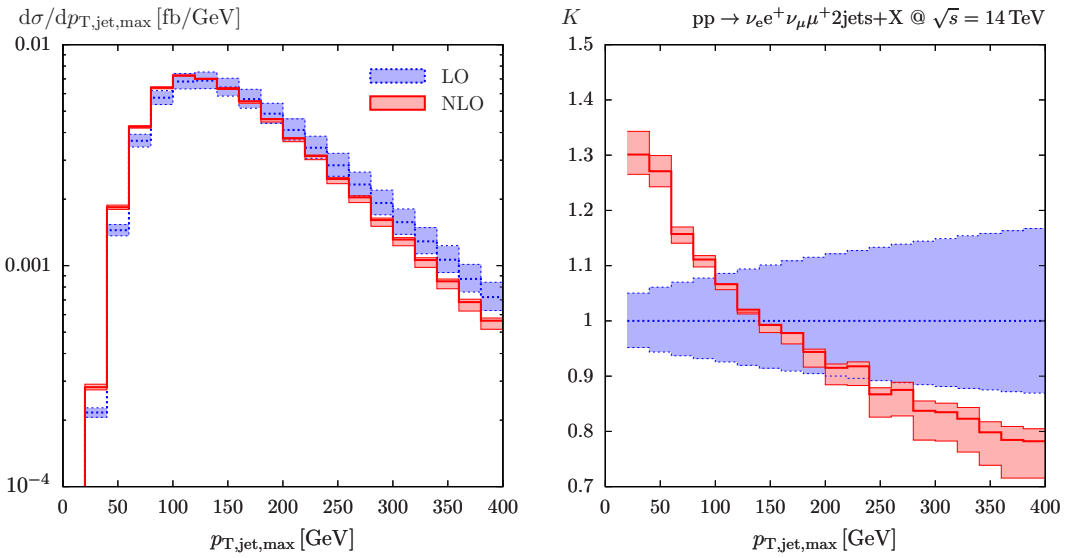

(a) $\mu_F = \mu_R = M_W$

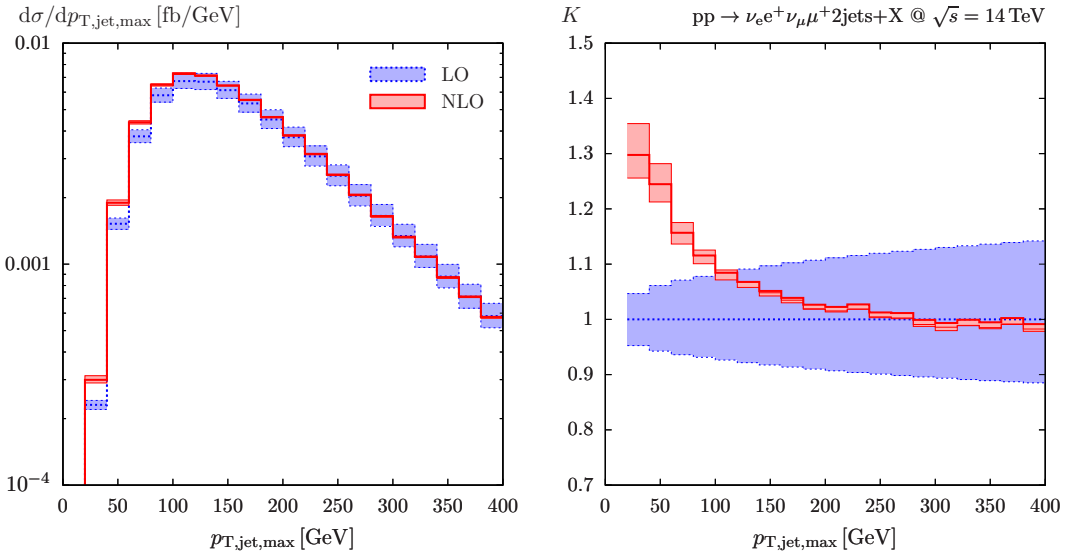

(b) $\mu_F = \mu_R = \sqrt{p_{T,jet_1} \cdot p_{T,jet_2}}$

Figure 3: Transverse momentum distribution of the tagging jet with the higher p_T for the fixed (a) and dynamic scale (b) on the left and the corresponding K factor represented by the solid (red) line on the right.

has been evaluated for three different sets of matrix elements as shown in Table 1. It confirms that σ^{LO}_{VBF} (containing only squares of t- and u-channel contributions but no interferences) can be considered a very good approximation of the full LO cross section, and the NLO cross section has therefore been evaluated using only t- and u-channel contributions without interferences between them in order to improve the speed of the calculation.

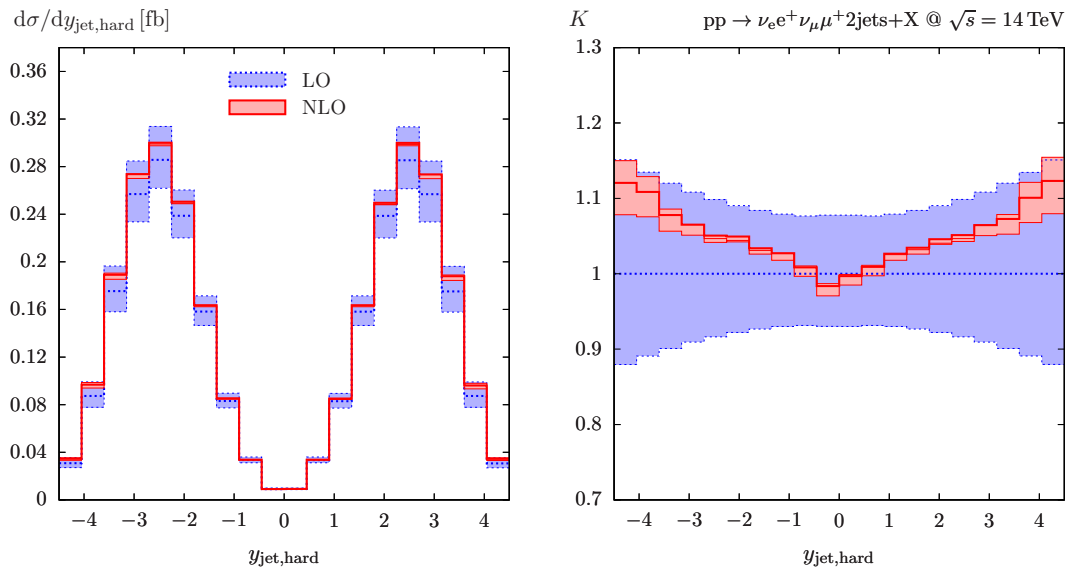

Figure 4: Absolute rapidity distribution for the harder tagging jet for the dynamic scale on the left and the corresponding K factor represented by the solid (red) line on the right.

$\sigma^{\text{LO}}_{\text{full}}$[fb]	$\sigma^{\text{LO}}_{\text{VBF+int}}$[fb]	$\sigma^{\text{LO}}_{\text{VBF}}$[fb]	$\sigma^{\text{NLO}}_{\text{VBF}}$[fb]
1.2224(2)	1.2218(2)	1.2230(2)	1.2917(8)

Table 1: Integrated cross sections for LO including all channels and interferences ($\sigma^{\text{LO}}_{\text{full}}$), for LO including t–u interferences, but neglecting s-channel diagrams ($\sigma^{\text{LO}}_{\text{VBF+int}}$), for LO in the VBF approximation, i.e. neglecting all s-channel diagrams and interferences ($\sigma^{\text{LO}}_{\text{VBF}}$), and for NLO in the VBF approximation ($\sigma^{\text{NLO}}_{\text{VBF}}$).

3.1 Differential distributions

Figure 3 shows the LO and NLO cross sections as a function of the transverse momentum of the harder of the two tagging jets. The distribution peaks at $p_{\text{T}} \sim 110\,\text{GeV}$, confirming the preference of the high-p_{T} regions by the VBF tagging jets. The plots on the right show the LO and NLO predictions normalized to the LO result at the central scale, i.e. $K_{\text{LO}}(\xi) = \text{d}\sigma_{\text{LO}}(\xi)/\text{d}\sigma_{\text{LO}}(\xi = 1)$ (dotted blue line), and $K_{\text{NLO}}(\xi) = \text{d}\sigma_{\text{NLO}}(\xi)/\text{d}\sigma_{\text{LO}}(\xi = 1)$ (solid red line). One can observe that $K(p_{\text{T,j}_{\text{max}}})$ grows noticeably in low-p_{T} regions for both FS and DS towards the value 1.3, while in the larger-p_{T} regions it drops to 0.8 in case of the FS (Figure 3a) and remains very close to 1 for the DS (Figure 3b), which is a behaviour that motivated the choice of the DS in the first place and can also be observed in other jet distributions.

Rapidity of the tagging jets is another distinguishing feature of the VBF processes since they exhibit very little jet activity in its central region, as shown in Figure 4. This is in sharp contrast to the behaviour of the QCD production mode for W^+W^+, where the jet rapidity peaks at 0, dominating the central rapidity region [15]. This process thus constitutes background which can be suppressed dramatically by imposing a cut on the separation of individual jet rapidities Δy_{jj}.

Acknowledgments

I would like to thank Ansgar Denner and Stefan Kallweit for their fruitful collaboration, and the theory groups at PSI and the University of Zurich for their hospitality. This work is supported in part by the European Commission through the Marie-Curie Research Training Network HEP-TOOLS under contract MRTN-CT-2006-035505, by the Research Executive Agency (REA) of the European Union under the Grant Agreement number PITN-GA-2010-264564 (LHCPhenoNet), by the Spanish Government and EU ERDF funds (grants FPA2007-60323, FPA2011-23778 and CSD2007-00042 Consolider Project CPAN) and by GV (PROMETEUII/2013/007).

References

[1] B. Jäger, C. Oleari, and D. Zeppenfeld, *Next-to-leading order QCD corrections to W^+W^+jj and W^-W^-jj production via weak-boson fusion*, *Phys. Rev.* **D80** (2009) 034022, [arXiv:0907.0580].

[2] A. Denner, L. Hošeková, and S. Kallweit, *NLO QCD corrections to W+ W+ jj production in vector-boson fusion at the LHC*, *Phys.Rev.* **D86** (2012) 114014, [arXiv:1209.2389].

[3] G. Bozzi, B. Jäger, C. Oleari, and D. Zeppenfeld, *Next-to-leading order QCD corrections to W^+Z and W^-Z production via vector-boson fusion*, *Phys. Rev.* **D75** (2007) 073004, [hep-ph/0701105].

[4] T. Hahn, *FormCalc 6*, *PoS* **ACAT08** (2008) 121, [arXiv:0901.1528].

[5] A. Denner and S. Dittmaier, *Reduction of one-loop tensor 5-point integrals*, *Nucl. Phys.* **B658** (2003) 175–202, [hep-ph/0212259].

[6] A. Denner and S. Dittmaier, *Reduction schemes for one-loop tensor integrals*, *Nucl. Phys.* **B734** (2006) 62–115, [hep-ph/0509141].

[7] A. Denner, U. Nierste, and R. Scharf, *A Compact expression for the scalar one loop four point function*, *Nucl. Phys.* **B367** (1991) 637–656.

[8] W. Beenakker and A. Denner, *Infrared Divergent Scalar Box Integrals with Applications in the Electroweak Standard Model*, *Nucl. Phys.* **B338** (1990) 349–370.

[9] A. Denner and S. Dittmaier, *Scalar one-loop 4-point integrals*, *Nucl.Phys.* **B844** (2011) 199–242, [arXiv:1005.2076].

[10] A. Denner, S. Dittmaier, and L. Hofer, "*COLLIER*, *Complex One-Loop Library In Extended Regularizations*." in preparation.

[11] S. Catani and M. H. Seymour, *A general algorithm for calculating jet cross sections in NLO QCD*, *Nucl. Phys.* **B485** (1997) 291–419, [hep-ph/9605323].

[12] A. Denner, S. Dittmaier, S. Kallweit, and S. Pozzorini, *NLO QCD corrections to off-shell top-antitop production with leptonic decays at hadron colliders*, *JHEP* **1210** (2012) 110, [arXiv:1207.5018].

[13] F. Cascioli, P. Maierhofer, and S. Pozzorini, *Scattering Amplitudes with Open Loops*, *Phys.Rev.Lett.* **108** (2012) 111601, [arXiv:1111.5206].

[14] J. Alwall, P. Demin, S. de Visscher, R. Frederix, M. Herquet, *et. al.*, *MadGraph/MadEvent v4: The New Web Generation*, *JHEP* **0709** (2007) 028, [arXiv:0706.2334].

[15] B. Jäger and G. Zanderighi, *NLO corrections to electroweak and QCD production of W^+W^+ plus two jets in the POWHEG BOX*, *JHEP* **1111** (2011) 055, [arXiv:1108.0864].